


Rapid Flipping of Parametric Phase States

Journal Article

Author(s):

Frimmer, Martin; Heugel, Toni L.; Nosan, Žiga; Tebbenjohanns, Felix; Hälgl, David; Akin, Abdulkadir; Degen, Christian L.; [Novotny, Lukas](#) ; Chitra, R.; Zilberberg, Oded; Eichler, Alexander

Publication date:

2019-12-20

Permanent link:

<https://doi.org/10.3929/ethz-b-000387859>

Rights / license:

[In Copyright - Non-Commercial Use Permitted](#)

Originally published in:

Physical Review Letters 123(25), <https://doi.org/10.1103/PhysRevLett.123.254102>

Funding acknowledgement:

163818 - Electronic and photonic quantum engineered systems (SNF)

Rapid Flipping of Parametric Phase States

Martin Frimmer,¹ Toni L. Heugel,² Žiga Nosan,³ Felix Tebbenjohanns,¹ David Hälgl,³ Abdulkadir Akin,³ Christian L. Degen,³ Lukas Novotny,¹ R. Chitra,² Oded Zilberberg,² and Alexander Eichler^{3,*}

¹Photonics Laboratory, ETH Zürich, CH-8093 Zürich, Switzerland

²Institute for Theoretical Physics, ETH Zürich, CH-8093 Zürich, Switzerland

³Laboratory for Solid State Physics, ETH Zürich, CH-8093 Zürich, Switzerland



(Received 7 June 2019; published 19 December 2019)

We experimentally demonstrate flipping the phase state of a parametron within a single period of its oscillation. A parametron is a binary logic element based on a driven nonlinear resonator. It features two stable phase states that define an artificial spin. The most basic operation performed on a parametron is a bit flip between these two states. Thus far, this operation involved changing the energetic population of the resonator and therefore required a number of oscillations on the order of the quality factor Q . Our technique takes a radically different approach and relies on rapid control of the underlying potential. Our work represents a paradigm shift for phase-encoded logic operations by boosting the speed of a parametron bit flip to its ultimate limit.

DOI: 10.1103/PhysRevLett.123.254102

Introduction.—Since the invention of the solid-state transistor, the overwhelming majority of computers followed the von Neumann architecture that strictly separates logic operations and memory [1,2]. Today, there is a revived interest in alternative computation models accompanied by the necessity to develop corresponding hardware architectures [3–6]. For example, phase-based logic architectures can be realized with artificial spins such as the parametron that arises in driven nonlinear resonators [7–17]. The parametron encodes binary information in the phase state of its oscillation. It enables, in principle, logic operations without energy transfer and the corresponding speed limitations [18].

The parametron is a logic device employing the principle of parametric driving [11,19–24]. Consider a resonator whose natural frequency f_0 is modulated at a drive frequency $2f_d$. If f_d is chosen close to f_0 , and the modulation is sufficiently strong, the resonator experiences a negative effective damping and is forced to oscillate at f_d with large amplitude, as illustrated in Fig. 1(a). With the frequency of the motion being half that of the modulation, the resonator undergoes a spontaneous time-translation symmetry breaking [25,26]. As a result, the system is locked to one of the two available phase states that are degenerate in amplitude but separated by π in phase (relative to a clock running at f_d). In phase space spanned by normalized displacement X and momentum Y [27], this locking mechanism can be illustrated by the quasipotential landscape shown in Fig. 1(b). The quasipotential features a double-well structure, where each well corresponds to a stable phase state. The two phase states of the parametron represent a classical bit or, analogously, an Ising spin. In the lab frame, the states rotate around the phase-space origin at the drive frequency f_d [Fig. 1(c)].

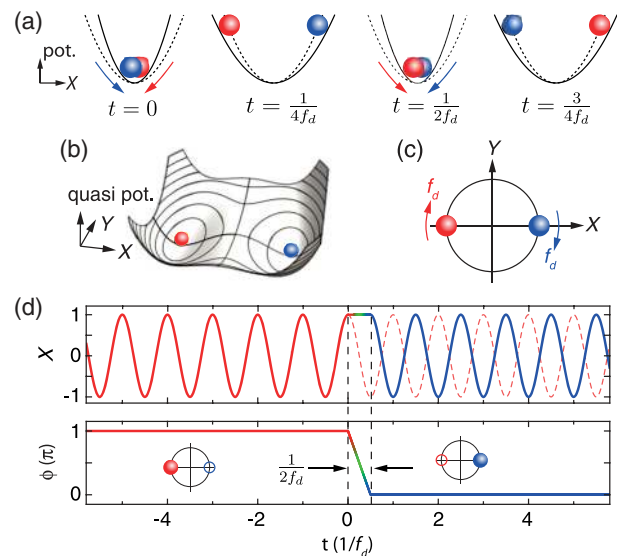


FIG. 1. Parametron phase states and basic idea of rapid phase flipping. (a) Parametric driving corresponds to a harmonic modulation of the resonator's natural frequency f_0 . Solid (dashed) lines represent the modulated (original) potential. If the drive is sufficiently strong, the resonator locks to f_d and settles into one of two stable phase states that are separated by π , illustrated as oscillating red and blue spheres. (b) In phase space, the parametrically driven resonator experiences an effective double-well potential, which is the key signature of the parametron. The phase states now appear as stationary red and blue spheres in the quasipotential minima. (c) Simplified illustration of the parametron in phase space. In the lab frame, the two states rotate around the origin at frequency f_d . (d) Illustration of rapid phase flip. The parametron is initialized in the red phase state ($\phi = \pi$). At time $t = 0$, the phase evolution of the system is paused for half an oscillation period by freezing the resonator's position. Upon release, the parametron resumes oscillation in the blue phase state ($\phi = 0$).

While the parametron was already patented at the dawn of the digital era [7,8], it is only with recent experimental advances that an implementation of the concept appears useful. Research groups using nanomechanical resonators, Josephson junction circuits, and optical parametric oscillators have devised prototypical parametron-based Ising machines that may solve nondeterministic polynomial-time-hard problems much faster than conventional computers [13–15,17,24,28]. The most basic logic operation on a parametron is a bit flip, corresponding to a phase change of π of the underlying resonator. Thus far, parametrons have been flipped by first depleting the resonator and then re-energizing it in the opposite phase state [13,21]. The flipping speed of this method is limited by the ring-down time $\tau = Q/(\pi f_0)$, where $Q \gg 1$ is the quality factor of the resonator. This speed limitation is directly related to the energy gap between energized and depleted states. However, flipping the phase state of a parametron does not strictly require energy transfer. Indeed, the two logic states are degenerate in energy and protected by a “phase gap” [18]. It should therefore be possible to devise a protocol to flip between the phase states at a speed much faster than the ringdown time τ , which is often (erroneously) deemed a fundamental limit for resonator operations [29,30]. Despite the fact that such a protocol would unlock the full potential of phase-encoded logic, an experimental demonstration has remained elusive to date.

In this Letter, we experimentally demonstrate flipping between the two phase states of a parametron within a single oscillation period. Our technique allows logic operations on a timescale of $1/f_0$, and therefore Q times faster than the ring-down time. Our protocol temporarily freezes (or slows down) the evolution of a resonator to bridge the phase gap separating its phase states. The speed of our method relies on the fact that it does not require energy transfer into or out of the system. The demonstrated protocols are platform independent. We present two complementary variations of our phase-flip paradigm on different experimental systems and assess their performances. Our results call for a reevaluation of the fundamental limits for high-speed and low-energy computation using parametron bits.

Phase-flip protocols.—The general idea for rapid parametron phase flipping is illustrated in Fig. 1(d). The resonator is initially in one of the two stable phase states. Without limitation of generality, let us consider the red phase state with phase $\phi = \pi$. At $t = 0$, the resonator evolution is frozen (or slowed down), such that it acquires a phase delay relative to its initial state. Careful timing results in a delay of exactly π . Upon release, the resonator resumes oscillation in the blue phase state with phase 0. In the following, we consider two methods to achieve such a phase delay by π . They make use of “potential deformation” and “potential displacement,” corresponding to a change in the restoring force and to the application of an external force, respectively.

Phase flip via potential deformation.—We first demonstrate rapid parametron phase flipping via potential deformation, corresponding to switching the underlying resonator’s natural frequency f_0 . As an experimental platform, we use a silica nanoparticle optically levitated in a focused laser beam in vacuum, as illustrated in Fig. 2(a) (see [31] and the Supplemental Material [32] for details). The light scattered by the particle provides us with a measurement of its position. Each degree of freedom of the particle’s center-of-mass represents a nonlinear resonator [36]. To minimize the effect of thermal fluctuations, we feedback-cool all three degrees of freedom to a temperature of 1 K. Throughout this Letter, we focus on a single oscillation mode with a resonance frequency $f_0 \sim 164$ kHz. The power spectral density of the feedback-cooled mode under consideration is shown in Fig. 2(b).

Weak periodic modulation of the trapping laser intensity turns the levitated particle into a parametron. In contrast, a sudden and strong reduction of the laser intensity leads to a deformation of the potential and can be used for phase flips. Consider the particle confined in a potential of natural frequency f_0 under parametric driving at $2f_d$ (with $f_d \sim f_0$), such that the parametron is locked to one of the two stable phase states [Figs. 2(c) and 2(d)]. When the particle reaches its maximum displacement (and its velocity vanishes), we reduce the power of the trapping laser to switch the natural oscillation frequency to $f_0/2$ for a time τ_{def} . If we choose $\tau_{\text{def}} = 1/f_0$, the particle has time to travel to the opposite side of the potential. At this moment, we switch the laser intensity (and thus the trap stiffness) back to its original value and the particle continues to oscillate at a frequency f_d . Importantly, relative to the clock at f_d , the phase state of the parametron has been flipped by π during the protocol.

We show an experimental demonstration of our idea in Fig. 2(e), where we plot the phase state of the optically levitated parametron as a function of time. The measurement signal is the output of a lock-in amplifier fed with the position signal. The trap frequency is switched twice per second from $f_0 = 164$ kHz to the reduced value 82 kHz for a duration $\tau_{\text{def}} = 8.1 \mu\text{s}$. Indeed, we observe two phase states separated by π and flipping between them at the expected rate of 2 Hz. The phase flips happen instantaneously on the timescale set by the 220 Hz bandwidth of our lock-in detection.

A striking feature in Fig. 2(e) is the failed phase flip around 8 s, indicating that the success probability P_{flip} of our potential deformation scheme is less than unity (we define P_{flip} as the ratio of observed phase flips to flipping attempts). We attribute this observation to the fact that we did not choose the nominally ideal value of $\tau_{\text{def}} = 6.1 \mu\text{s}$. To corroborate this hypothesis, we record P_{flip} for varying τ_{def} . In Fig. 2(f), we observe that P_{flip} is indeed a periodic function of τ_{def} with the expected period $2/f_d$. When τ_{def} is an even multiple of $1/f_d$, the parametron phase remains unaltered by the pulse and P_{flip} vanishes. In contrast, for

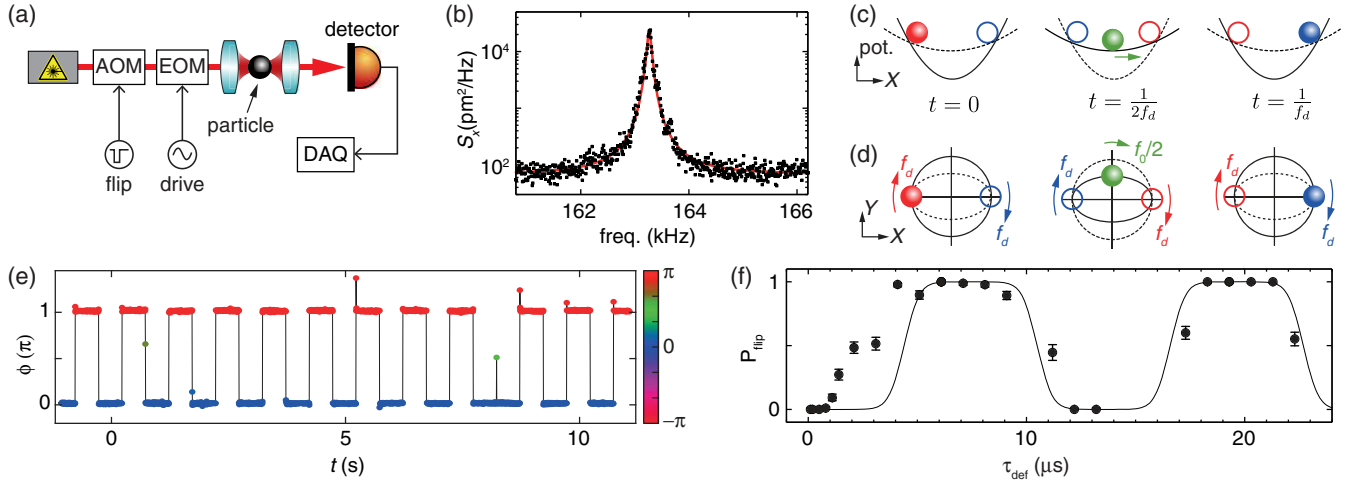


FIG. 2. Experimental demonstration of phase flip via potential deformation. (a) Experimental setup. A silica nanoparticle (diameter 136 nm) is trapped in a focused laser beam (wavelength 1064 nm) inside a vacuum chamber (not shown). The stiffness of the optical potential can be modulated with an electro-optic modulator (EOM). The particle displacement is detected with a quadrant photo diode (QPD). (b) Thermally driven power spectral density S_x of the particle displacement. From the red line fit, we extract a quality factor $Q = 1970$. (c) Schematic illustration of the phase-flip protocol. The parametron is initialized in the red phase state. When the particle reaches its maximum displacement, we reduce the resonator frequency from f_0 (potential sketched as solid line) to $f_0/2$ (dashed line) by attenuating the laser intensity with an acousto-optic modulator (AOM). We then let the particle evolve for the pulse length $\tau_{\text{def}} = 1/f_0$, such that the phase states of the parametron undergo a full oscillation, while the particle only traverses the trap and acquires a phase delay of π . (d) Same as (c) but illustrated in phase space. (e) Measured phase of the parametron as a function of time. A switch of the potential as outlined in (c) and (d) is applied at a rate of 2 Hz with $\tau_{\text{def}} = 8.1 \mu\text{s}$, periodically flipping the parametron phase state. Note the failed flip around 8 s. (f) Flipping probability P_{flip} for varying pulse length τ_{def} . Our model (black line) takes into account the finite thermal population of the resonator (see the Supplemental Material [32]). Error bars represent statistical uncertainty.

τ_{def} equal to an odd multiple of $1/f_d$, P_{flip} approaches unity. We note that a pulse of length $\tau_{\text{def}} = 2/f_d$ can be interpreted as a sequence of two back-to-back pulses of length $1/f_d$. The data in Fig. 2(f) therefore demonstrate that it is possible to fully exploit the switching speed of our method by concatenating several rapid phase-flips.

Figure 2(f) reveals that the transitions of $P_{\text{flip}}(\tau_{\text{def}})$ between zero and unity are not infinitely sharp but display a finite width of about $2 \mu\text{s}$, which we attribute to thermo-mechanical fluctuations. The solid line in Fig. 2(f) indicates a model calculation of P_{flip} based on thermal phase noise (see the Supplemental Material [32]). This model reproduces our data well for $\tau_{\text{def}} > 5 \mu\text{s}$. We attribute the deviations between data and model for short τ_{def} to the finite response time and the resulting transients of the modulator that switches the laser power.

We note that in our experiment, we triggered a phase flip when the resonator displacement was at its maximum. The protocol is, however, applicable with any starting condition (see the Supplemental Material [32]). Indeed, under the applied potential deformation, a harmonic oscillator with initial phase state (X, Y) will always evolve towards $-(X, Y)$ within half a period. By extension, the protocol is applicable to arbitrary mixtures of states, including thermal states. Finally, we point out that the flipping time of our protocol could be further reduced to $1/(2f_d)$ by completely turning off the trapping potential. For our

particular experimental situation, switching off the potential also reduces the parametric drive to zero. On the short timescale of the flipping process, this is not problematic because parametric locking is only effective on time scales of the order of τ . However, the scheme implemented in this work is significantly more resilient against inevitable thermal fluctuations of the particle motion which can lead to particle loss.

Phase flip via potential displacement.—In the following, we demonstrate that rapid parametron phase flips are also possible by displacing the potential, corresponding to the application of a force to the resonator. We experimentally realize this method with the electrical LC circuit illustrated in Fig. 3(a) (see [37] and the Supplemental Material [32] for details). Here, the resonator displacement corresponds to the charge separated across the varicap diode with capacitance C , and the role of the force is assumed by a voltage U_{flip} . We characterize our resonator in the linear regime by applying a weak drive tone U_{drive} whose frequency we sweep around f_0 while recording the output voltage U_{meas} , as shown in Fig. 3(b). The circuit becomes a parametron under sufficiently strong driving close to $2f_0$.

We use this system to realize the phase-flipping scheme detailed in Figs. 3(c) and 3(d). When the resonator displacement reaches its maximum value, a force is applied to counter the restoring force and to freeze the resonator evolution. This equals a displacement of the potential by

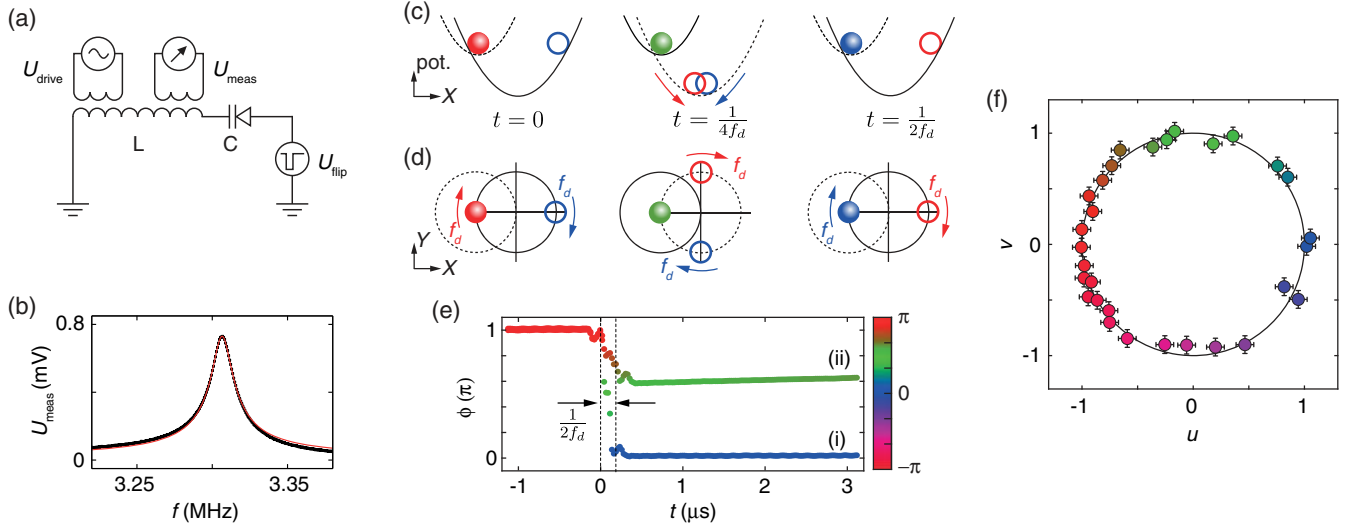


FIG. 3. Experimental demonstration of phase flips via potential displacement. (a) Schematic of the electrical LC resonator circuit with a varicap diode to provide a nonlinear capacitance C . (b) Linear response of the resonator to a small external driving voltage ($U_{\text{drive}} = 50$ mV). From the red line fit we extract $f_0 = 3.3$ MHz and $Q = 245$. (c) Illustration of the phase-flip protocol. The parametron is initialized in the red phase state. When the resonator reaches its maximum displacement at $t = 0$, the potential is displaced by an external force (from dashed to solid lines) such that the resonator is momentarily at rest. At $t = 1/(2f_d)$, the force is turned off and the parametron resumes its evolution, now in the blue phase state. (d) Same as (c) but illustrated in phase space. (e) Demonstration of two different phase flips, performed with (i) $\tau_{\text{dis}} = 153$ ns, the ideal pulse duration for flipping, and with (ii) $\tau_{\text{dis}} = 230$ ns. The signal was demodulated by a digital lock-in amplifier and filtered for clarity (see the Supplemental Material [32]). (f) Results of flipping experiments with varying τ_{dis} . Each datapoint represents the state of the resonator directly after a pulse. Here, $u = X \cos(2\pi f_d t) - Y \sin(2\pi f_d t)$ and $v = Y \cos(2\pi f_d t) + X \sin(2\pi f_d t)$ are the phase-space quadratures in a frame rotating at the drive frequency f_d . A black circle serves as a guide to the eye.

the oscillation amplitude, such that the resonator temporarily finds itself at the potential center. After the force is turned off, the resonator has acquired a phase delay of π relative to its original evolution and is stable in the opposite phase state.

In Fig. 3(e), we show two examples of the behavior of the system for different pulse lengths τ_{dis} . In the first example, the pulse length is set to $\tau_{\text{dis}} = 1/(2f_0)$, the ideal pulse length for a bit flip. Indeed, the parametron flips its phase state by π (i, blue data points). In the second example, we set $\tau_{\text{dis}} = 1.5 \times 1/(2f_0)$ (ii, green). Here, the parametron is transferred into a state between the two stable phase states and evolves towards one of them on a timescale given by $Q/f_0 \sim 74 \mu\text{s}$ after the flip.

In Fig. 3(f), we plot the state of the resonator at $t = 0.7 \mu\text{s}$ after the start of a bit flip in phase space (in a frame rotating at the drive frequency) for different values of τ_{dis} . The amplitude of the parametron after the flipping protocol (corresponding to the radial distance from the plot center) is independent of τ_{dis} , which results from the fact that the resonator's evolution is frozen at the point of maximum displacement and vanishing velocity. Our data demonstrate that via the choice of τ_{dis} we can transfer the parametron to any point on the unit circle in phase space, in particular to the two stable phase states.

Discussion and conclusion.—The two experimental demonstrations in Figs. 2 and 3 establish a new paradigm for

resonator-based logic operations. Parametron phase flips can be achieved within a single oscillation period and completely independently from the quality factor Q . This finding opens up new possibilities for applications that use parametrons as phase logic units [7–9, 11–14, 16, 17, 38–41]. The states of the parametrons may be initialized and flipped irrespective of the (desirable) high quality factors of the underlying resonators, and the flips do not necessarily involve energy exchange with a bath. In this way, our schemes reconcile the two seemingly disparate notions of rapid logic operations and long state coherence [42, 43]. Beyond computation, rapid phase flips allow encoding binary information through phase-shift keying [44]. While current phase-shift keying techniques use an oscillator with constant amplitude and phase and achieve different phase-space states through postprocessing, our demonstrations show that information encoding on the level of the resonator itself is feasible. This may enable ultracompact and low-power encoders for specialized applications such as autonomous nanobots in medical research [45, 46].

There are several factors that significantly relax the required conditions for large-scale implementations of our technique. First, the symmetry protection of the parametron makes the phase-flips very stable in the presence of phase noise [18]. Consecutive rapid flips result in the correct state as long as the summed phase error is below

$\pi/2$. After a sequence of rapid flips, phase errors will self-correct through relaxation within the double-well. Second, the external parametric driving signal can be utilized as a clock with large signal-to-noise ratio. Estimating the momentary state of a parametron is thus fault tolerant up to $\pi/2$, while the amplitude is generally known.

The physics explored within our work may be translated to nonlinear high-frequency resonators based on Josephson junction circuits [17,22–24], micro- and nanomechanical resonators such as carbon nanotube and graphene devices [21,23,47–51], optical parametric oscillators in nonlinear media [12,14,28], trapped ions [52], and cold atom lattices [53]. It is thus a highly general concept that is potentially useful in a wide variety of experiments and future applications.

We are indebted to Peter Märki, Nils Hauff, David Ruffieux, and Can Knaut for valuable discussions and technical assistance during this project. This research was supported by ERC-QMES (Grant No. 338763), the NCCR-QSIT program (Grant No. 51NF40-160591), the Swiss National Science Foundation (CRSII5 177198/1, PP00P2_163818), the Michael Kohn Foundation, the ETH Zürich Foundation, and a Public Scholarship of the Development, Disability and Maintenance Fund of the Republic of Slovenia (11010-247/2017-12).

* eichlera@phys.ethz.ch

- [1] J. von Neumann, *IEEE Ann. Hist. Comput.* **15**, 27 (1993).
 [2] M. D. Godfrey and D. F. Hendry, *IEEE Ann. Hist. Comput.* **15**, 11 (1993).
 [3] S. Kirkpatrick, C. D. Gelatt, and M. P. Vecchi, *Science* **220**, 671 (1983).
 [4] F. C. Hoppensteadt and E. M. Izhikevich, *Phys. Rev. Lett.* **82**, 2983 (1999).
 [5] I. M. Georgescu, S. Ashhab, and F. Nori, *Rev. Mod. Phys.* **86**, 153 (2014).
 [6] G. Carleo and M. Troyer, *Science* **355**, 602 (2017).
 [7] E. Goto, *Proc. IRE* **47**, 1304 (1959).
 [8] J. v. Neumann, U.S. Patent No. 2815488 (1959).
 [9] F. Sterzer, *Proc. IRE* **47**, 1317 (1959).
 [10] M. Hosoya, W. Hioe, J. Casas, R. Kamikawai, Y. Harada, Y. Wada, H. Nakane, R. Suda, and E. Goto, *IEEE Trans. Appl. Supercond.* **1**, 77 (1991).
 [11] I. Mahboob, E. Flurin, K. Nishiguchi, A. Fujiwara, and H. Yamaguchi, *Nat. Commun.* **2**, 198 (2011).
 [12] Z. Wang, A. Marandi, K. Wen, R. L. Byer, and Y. Yamamoto, *Phys. Rev. A* **88**, 063853 (2013).
 [13] I. Mahboob, H. Okamoto, and H. Yamaguchi, *Sci. Adv.* **2**, e1600236 (2016).
 [14] T. Inagaki, K. Inaba, R. Hamerly, K. Inoue, Y. Yamamoto, and H. Takesue, *Nat. Photonics* **10**, 415 (2016).
 [15] H. Goto, *Sci. Rep.* **6**, 21686 (2016).
 [16] G. Csaba, T. Ytterdal, and W. Porod, in *2016 IEEE International Conference on Electronics, Circuits and Systems (ICECS)* (IEEE, New York, 2016), pp. 45–48.
 [17] S. Puri, S. Boutin, and A. Blais, *npj Quantum Inf.* **3**, 18 (2017).
 [18] J. Roychowdhury, *Proc. IEEE* **103**, 1958 (2015).
 [19] M. I. Dykman, C. M. Maloney, V. N. Smelyanskiy, and M. Silverstein, *Phys. Rev. E* **57**, 5202 (1998).
 [20] M. C. Lifshitz and R. Cross, Nonlinear dynamics of nanomechanical and micromechanical resonators, in *Reviews of Nonlinear Dynamics and Complexity* (Wiley-VCH, Weinheim, 2009), pp. 1–52.
 [21] I. Mahboob and H. Yamaguchi, *Nat. Nanotechnol.* **3**, 275 (2008).
 [22] C. M. Wilson, T. Duty, M. Sandberg, F. Persson, V. Shumeiko, and P. Delsing, *Phys. Rev. Lett.* **105**, 233907 (2010).
 [23] M. Dykman, *Fluctuating Nonlinear Oscillators* (Oxford University Press, New York, 2012).
 [24] Z. Lin, K. Inomata, K. Koshino, W. D. Oliver, Y. Nakamura, J. S. Tsai, and T. Yamamoto, *Nat. Commun.* **5**, 4480 (2014).
 [25] F. Wilczek, *Phys. Rev. Lett.* **109**, 160401 (2012).
 [26] A. Leuch, L. Papariello, O. Zilberberg, C. L. Degen, R. Chitra, and A. Eichler, *Phys. Rev. Lett.* **117**, 214101 (2016).
 [27] I. I. Rabi, N. F. Ramsey, and J. Schwinger, *Rev. Mod. Phys.* **26**, 167 (1954).
 [28] A. Marandi, Z. Wang, K. Takata, R. L. Byer, and Y. Yamamoto, *Nat. Photonics* **8**, 937 (2014).
 [29] R. Budakian, H. J. Mamin, and D. Rugar, *Appl. Phys. Lett.* **89**, 113113 (2006).
 [30] N. Liu, F. Giesen, M. Belov, J. Losby, J. Moroz, A. E. Fraser, G. McKinnon, T. J. Clement, V. Sauer, W. K. Hiebert, and M. R. Freeman, *Nat. Nanotechnol.* **3**, 715 (2008).
 [31] J. Gieseler, B. Deutsch, R. Quidant, and L. Novotny, *Phys. Rev. Lett.* **109**, 103603 (2012).
 [32] See the Supplemental Material <http://link.aps.org/supplemental/10.1103/PhysRevLett.123.254102> for experimental details, a model of the bit flip success rate, as well as Fokker-Planck numerical simulations, which includes Refs. [33–35].
 [33] C. Gardiner, *Stochastic Methods* (Springer-Verlag Berlin Heidelberg, Berlin, 2009).
 [34] J. Gieseler, R. Quidant, C. Dellago, and L. Novotny, *Nat. Nanotechnol.* **9**, 358 (2014).
 [35] V. Jain, J. Gieseler, C. Moritz, C. Dellago, R. Quidant, and L. Novotny, *Phys. Rev. Lett.* **116**, 243601 (2016).
 [36] J. Gieseler, L. Novotny, and R. Quidant, *Nat. Phys.* **9**, 806 (2013).
 [37] Z. Nosan, P. Märki, N. Hauff, C. Knaut, and A. Eichler, *Phys. Rev. E* **99**, 062205 (2019).
 [38] S. Puri, C. K. Andersen, A. L. Grimsmo, and A. Blais, *Nat. Commun.* **8**, 15785 (2017).
 [39] A. Yamamura, K. Aihara, and Y. Yamamoto, *Phys. Rev. A* **96**, 053834 (2017).
 [40] P. Zhao, Z. Jin, P. Xu, X. Tan, H. Yu, and Y. Yu, *Phys. Rev. Applied* **10**, 024019 (2018).
 [41] H. Goto, Z. Lin, and Y. Nakamura, *Sci. Rep.* **8**, 7154 (2018).
 [42] Y. Tsaturyan, A. Barg, E. S. Polzik, and A. Schliesser, *Nat. Nanotechnol.* **12**, 776 (2017).
 [43] A. H. Ghadimi, S. A. Fedorov, N. J. Engelsen, M. J. Berekhi, R. Schilling, D. J. Wilson, and T. J. Kippenberg, *Science* **360**, 764 (2018).

- [44] T. Rappaport, *Wireless Communications: Principles and Practice*, 2nd ed. (Prentice Hall PTR, New York, 2001).
- [45] R. Duncan and R. Gaspar, *Mol. Pharmaceutics* **8**, 2101 (2011).
- [46] J. Li, B. Esteban-Fernández de Ávila, W. Gao, L. Zhang, and J. Wang, *Sci. Robotics* **2**, 1 (2017).
- [47] D. Rugar and P. Grütter, *Phys. Rev. Lett.* **67**, 699 (1991).
- [48] R.B. Karabalin, S.C. Masmanidis, and M.L. Roukes, *Appl. Phys. Lett.* **97**, 183101 (2010).
- [49] L. G. Villanueva, R. B. Karabalin, M. H. Matheny, E. Kenig, M. C. Cross, and M. L. Roukes, *Nano Lett.* **11**, 5054 (2011).
- [50] A. Eichler, J. Chaste, J. Moser, and A. Bachtold, *Nano Lett.* **11**, 2699 (2011).
- [51] J.P. Mathew, R. N. Patel, A. Borah, R. Vijay, and M. M. Deshmukh, *Nat. Nanotechnol.* **11**, 747 (2016).
- [52] S. Ding, G. Maslennikov, R. Hablützel, H. Loh, and D. Matsukevich, *Phys. Rev. Lett.* **119**, 150404 (2017).
- [53] A. Schilke, C. Zimmermann, P.W. Courteille, and W. Guerin, *Nat. Photonics* **6**, 101 (2012).

Supplementary Material: Rapid flipping of parametric phase states

Martin Frimmer,¹ Toni L. Heugel,² Žiga Nosan,³ Felix Tebbenjohanns,¹ David Hälg,³ Abdulkadir Akin,³ Christian L. Degen,³ Lukas Novotny,¹ R. Chitra,² Oded Zilberberg,² and Alexander Eichler^{3,*}

¹Photonics Laboratory, ETH Zürich, CH-8093 Zürich, Switzerland.[†]

²Institute for Theoretical Physics, ETH Zürich, CH-8093 Zürich, Switzerland.

³Laboratory for Solid State Physics, ETH Zürich, CH-8093 Zürich, Switzerland.

(Dated: Monday 25th November, 2019)

S1. EXPERIMENTAL DETAILS: OPTICAL TRAPPING SETUP

We implement the bitflip based on a deformation of the potential using an optically trapped nanoparticle [S1]. An extended sketch of the setup is shown in Fig. S1. In our experiment, we focus a linearly polarized laser beam (wavelength 1064 nm, focal power 80 mW) with a microscope objective (0.8NA) inside a vacuum chamber. A dielectric nanoparticle (silica, diameter 136 nm) is trapped by the optical gradient force in the laser focus. We collect the light scattered by the particle in the forward direction, where it interferes with the transmitted trapping beam, and send it to a standard four-quadrant detection scheme. We can therefore monitor the particle's motion along all three coordinate axes as a function of time. We call the optical axis the z direction, while the x and y axes lie in the focal plane with the x axis perpendicular to the polarization direction. The center-of-mass motion of the particle resembles three Duffing oscillators [S2]. Our experiments take place at 5×10^{-6} mbar, where the particle's motion is strongly underdamped. We use parametric feedback cooling to reduce the thermal oscillation amplitude of the particle along all three axes to 1 K [S3]. At these low oscillation amplitudes any non-linear mode coupling is negligible. The feedback signal is derived from the position measurement using a phase-locked loop whose output is frequency doubled and whose phase is adjusted to achieve cooling. This feedback signal is applied to an electro-optic modulator (EOM). Throughout this work, we focus on the x mode of the particle with natural frequency $f_0 \approx 164$ kHz.

Under parametric driving at a frequency $2f_d$ (with f_d close to the natural frequency f_0), the particle motion locks to the drive and acquires a large oscillation amplitude [S4]. Driving the x mode leaves the remaining degrees of freedom essentially

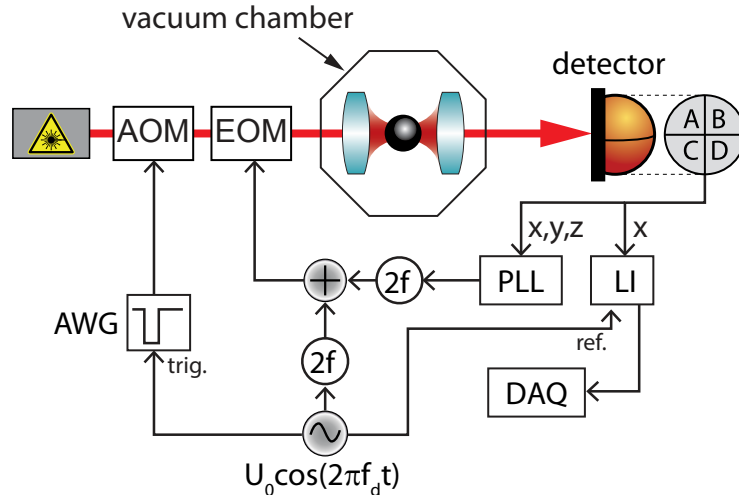


Figure S1: Experimental setup for phase flips via potential deformation.

*Electronic address: eichlera@phys.ethz.ch

[†]URL: <http://www.photonics.ethz.ch>

unaffected due to the large frequency difference between the modes ($f_z \approx 50$ kHz, $f_y \approx 130$ kHz). The parametric driving in our experimental system corresponds to a harmonic modulation of the laser intensity which sets the stiffness of the optical trap. We realize this parametric driving using the same EOM used for feedback cooling. The parametric driving signal is the frequency doubled output of a function generator producing a harmonic tone at f_d .

To effect the potential deformation leading to the flip of the parametron phase, we reduce the stiffness of the optical potential using an acousto-optic modulator (AOM). We have calibrated the device to switch the potential to half of the original stiffness by observing the natural frequency of the particle oscillation mode as a function of voltage applied to the AOM. To carry out a bitflip, we generate a square pulse of length τ_{def} with an arbitrary waveform generator (AWG). In order to effect the potential deformation at the desired time, we trigger the AWG by the parametric drive f_d to which the particle motion is locked in phase.

We extract the phase of the parametron by demodulating the detector signal of the measured particle position $x(t)$ at the drive frequency f_d using a lock-in amplifier (LI). The demodulated output of the LI is recorded by a data acquisition card (DAQ). A typical time trace of the phase output of the LI is shown in Fig. 2e of the main text. The timing resolution in this experiment is given by the bandwidth of the lock-in amplifier, which is chosen at 220 Hz in the presented experiments and is limited by the signal-to-noise ratio of the position measurement. With this timing resolution, the phase flips appear as essentially instantaneous in Fig. 2e and it is not possible to generate a highly time-resolved measurement of the phase as shown in Fig. 3e for the experiment with the LC resonator (which offers a dramatically higher signal-to-noise ratio). To gain information about the dynamics of the phase flip with higher timing resolution, we have devised the experiment shown in Fig. 2f. Here, our sub-microsecond control over the pulse length τ_{def} (provided by the waveform generator), allows us to investigate the dynamics of the phase flip on the timescale set by the natural frequency of the underlying resonator.

S2. MODEL FOR BIT-FLIP SUCCESS RATE

In this section, we describe the model giving rise to the solid line in Fig. 2f of the main text. Naively, one would expect P_{flip} to be a periodic rectangular function of τ_{def} , since the parametron will settle into the phase state $\phi = 0$ ($\phi = \pi$) if the deformation pulse takes it to a phase value in the range $[-\pi/2 \dots \pi/2]$ ($[\pi/2 \dots, 3\pi/2]$). However, Fig. 2(f) reveals that the transitions of $P_{\text{flip}}(\tau_{\text{def}})$ between zero and unity are not infinitely sharp but display a finite width of about $2 \mu\text{s}$, which we attribute to thermomechanical fluctuations.

To model our system, we describe the phase-space distribution of the parametron as a thermally broadened coherent state with a Gaussian probability distribution. The width of this Gaussian is determined by the temperature of the nanoparticle's center-of-mass motion. Under feedback cooling, the root-mean squared amplitude due to thermal activation is around 2 nm. The displacement of the Gaussian from the origin by the coherent drive amounts to 7 nm. When the trapping potential is deformed to have natural frequency $f_0/2$, the phase-space distribution rotates around the origin at that frequency. We calculate the bit-flip success rate $P_{\text{flip}}(\tau_{\text{def}})$ as the fraction of the phase-space distribution falling into the halfspace with negative amplitude X , given that the system was started with its phase-space distribution initially centered on the positive X axis. The resulting (appropriately normalized) variation of the complementary error function is plotted in Fig. 2f as a solid line. We note that the width of the transitions from zero to unity is given by the ratio of the amplitude due to the thermal drive relative to the thermal population. Both these quantities were independently measured. The period of the undulations of P_{flip} is given by $f_0/2$, and a fixed parameter as well. The only free parameter we allow for is a phase shift corresponding to a temporal delay of $1.3 \mu\text{s}$ to account for the finite response time of our AOM switching the trapping potential.

S3. EXPERIMENTAL DETAILS: ELECTRICAL RESONATOR SETUP

In Fig. S2, we show the full electrical schematic of the experiment used for rapid phase flipping with the potential displacement method. Calibration measurements for this setup were performed in a previous study [S5]. A tuning voltage $U_{\text{tune}} \sim 2$ V is used to bring the diode into reverse bias, and a second (large) capacitance $C_1 = 47$ nF prevents DC currents from flowing withing the resonator.

For every flipping event, we first switch on the driving voltage U_{drive} to drive the resonator into parametric resonance and lock it to the drive. At the same time, the lock-in amplifier (HF2LI by Zurich Instruments) sends a clock signal phase-locked to U_{drive} to the FPGA. After waiting for the resonator to reach a steady state ($t_{\text{wait}} \geq 0.2$ s), we measure its phase state relative to the clock.

In the next step of the phase-flipping protocol, we use a RedPitaya FPGA to detect a zero-crossing of the clock signal. The FPGA then outputs a single rectangular pulse after a calibrated delay that depends on the measured resonator phase. This pulse triggers the lock-in amplifier to start logging U_{meas} , and is at the same time the 'force' applied to the resonator with an additional delay Δt (this delay ensures that the measurement captures the entire flipping process). We use an operational amplifier (THS4271D) to preserve a high quality factor of the resonator and to enable a rapid switch of U_{flip} . The measured resonator

response U_{meas} is measured as a time trace and later post-processed digitally in a computer. After the flipping event, the phase of the resonator is measured once more by the lock-in amplifier to verify a successful phase reversal.

For each phase flip event, we run the raw signal through a digital lock-in amplifier at f_d to obtain the phase space quadratures. We then perform a fast Fourier transform (FFT) and apply a SINC filter with a cut-off frequency at f_d to eliminate unwanted harmonic responses. After a back-transformation into the time domain, we calculate the phase ϕ that is shown in Fig. 3e.

S4. THEORY DETAILS: FOKKER-PLANCK SIMULATIONS OF RAPID FLIPPING

In the following, we numerically investigate the robustness of the switching protocol based on the potential-deformation method. In particular, we demonstrate that the flipping fidelity of the potential-deformation method is independent of the time when the switch is executed within the parametron oscillation cycle. We perform these investigations using numerical simulations of corresponding time-dependent Fokker-Planck equations [S6].

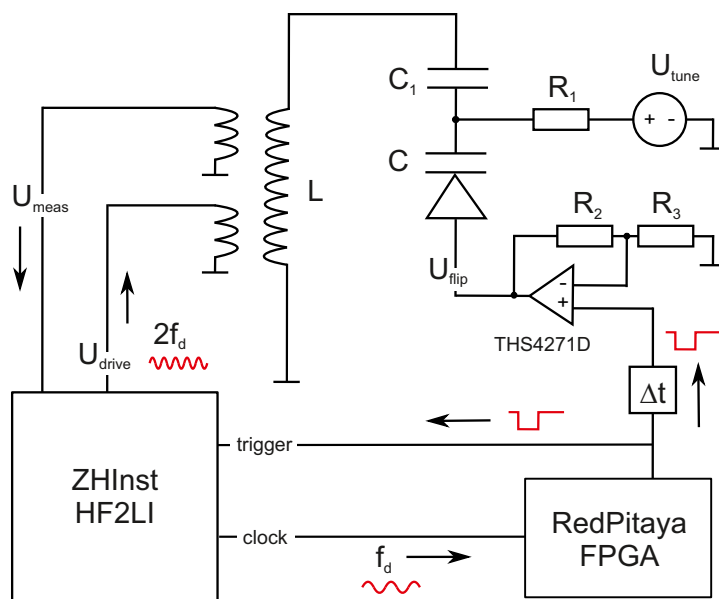


Figure S2: Experimental setup for phase flips via potential displacement.

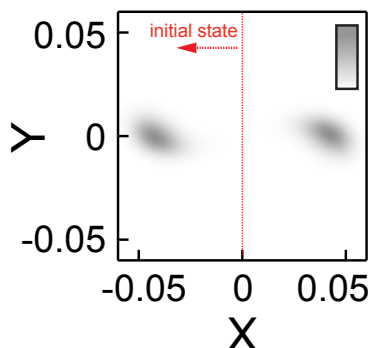


Figure S3: Probability density function (PDF) $p(X, Y, t)$ of the parametron's steady state for our simulation parameters. The colorbar ranges from $p = 0$ (white) to $p = 2425$ (grey). The integration of p over the entire phase space yields unity. We use the phase-space population in the half space $X < 0$ as the initial state for simulations of the bit-flip protocols.

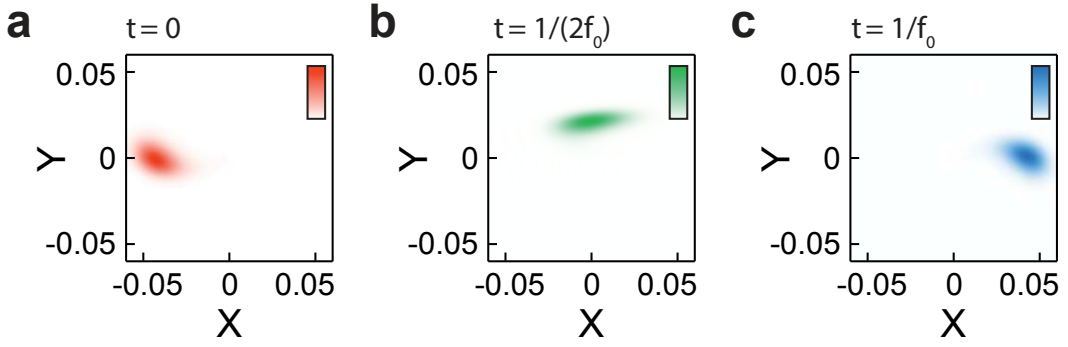


Figure S4: Fokker-Planck simulation of the potential-deformation protocol with noise. The bit-flip is initialized when the resonator has maximum (negative) displacement and minimum momentum. The three subfigures are snapshots of the flipping process at different times during the protocol and correspond to the three situations shown in Fig. 2d of the main text. The colorbars range from $p = 0$ (white) to $p = 4850$ (red/green/blue). (a) Initial state $p(X, Y, t = 0)$, corresponding to the steady state in Fig. S3 in the region $X < 0$ of phase space. (b) Probability density function (PDF) of the parametron in the middle of the flipping protocol, corresponding to time $t = 1/(2f_0)$. (c) PDF of the parametron at the end of the flipping protocol at time $t = 1/f_0$.

A. Details of the numerical model

In our analysis, we consider a nonlinear parametric resonator with additive force noise (originating, e.g., from thermal processes or from a noisy pulse). Our model can describe both experimental platforms used in this work (see [S5] and [S4]). We choose to discuss our model in the form of a mechanical resonator described by the equation of motion

$$\ddot{X} + \frac{\gamma}{m}\dot{X} + \omega_0^2 [1 - \lambda \cos(2\omega_d t)] X + \frac{\alpha}{m} X^3 = \frac{F(t)}{m} + \frac{\sigma \xi(t)}{m}. \quad (\text{S1})$$

Here, X is the displacement, $Y = \dot{X}$ the velocity, dots indicate differentiation with respect to time t , m is the effective mass, $\omega_0 = 2\pi f_0$ is the angular resonance frequency, $\gamma = m\omega_0/Q$ is a damping term, and α describes the strength of a cubic restoring force. The system is subject to a parametric drive with modulation depth λ at a rate $\omega_d = 2\pi f_d$. Deterministic external forces are summed up as $F(t)$. Stochastic forces are described by the noise intensity σ and the white noise process $\xi(t)$ with $\langle \xi(t) \rangle = 0$ and $\langle \xi(t)\xi(t') \rangle = \delta(t - t')$, where $\delta(t)$ is a Dirac-delta distribution.

The system can be described by the following Fokker-Planck equation for the probability density function (PDF) $p(X, Y, t)$ of finding the system at the phase-space point (X, Y) at time t . We rewrite Eq. (S1) as two coupled first order differential equations to obtain

$$\dot{X} = Y, \quad (\text{S2})$$

$$\dot{Y} = \frac{1}{m} \{ F(t) - \gamma Y - m\omega_0^2 [1 - \lambda \cos(2\omega_d t)] X - \alpha X^3 \} + \frac{\sigma}{m} \xi(t). \quad (\text{S3})$$

The Fokker-Planck equation for $p(X, Y)$ is then given by [S6]

$$\begin{aligned} \frac{\partial}{\partial t} p(X, Y, t) = & -Y \frac{\partial}{\partial X} p(X, Y, t) - \frac{1}{m} \frac{\partial}{\partial Y} \{ F(t) - \gamma Y - m\omega_0^2 X [1 - \lambda \cos(2\omega_d t)] - \alpha X^3 \} p(X, Y, t) \\ & + \frac{\sigma^2}{2m^2} \frac{\partial^2}{\partial Y^2} p(X, Y, t). \end{aligned} \quad (\text{S4})$$

For all following calculations, we use the dimensionless parameters $m = 1$, $Q = 1000$, $\omega_0 = \omega_d = 1$, $\lambda = 0.003$, $\alpha = 1$, $F = 0$ and $\sigma = 2.4 \times 10^{-4}$.

In a first step, we find the steady-state probability distribution p_{steady} of the parametron, see false-color plot in Fig. S3. The distribution p_{steady} features appreciable values only in two distinct lobes in (X, Y) phase space. These two regions correspond to the two stable phase states of the parametron and differ in phase by π as expected. The width of the two lobes is given by the magnitude of the fluctuating forces σ together with the damping rate γ , while the radial distance of the lobes' respective centers from the phase-space origin is set by the driving strength λ and the non-linearity parameter α . In order to investigate the behavior of the phase-space distribution under our bit-flip protocols, we use as an initial distribution p_{ini} the part of p_{steady} residing in the half of phase space with $X < 0$. In other words, to obtain p_{ini} , we set p_{steady} to zero in the region $X > 0$ and renormalize the amplitude. In the following, we investigate the phase-space distribution $p(X, Y, t)$ after execution of a phase-flip protocol.

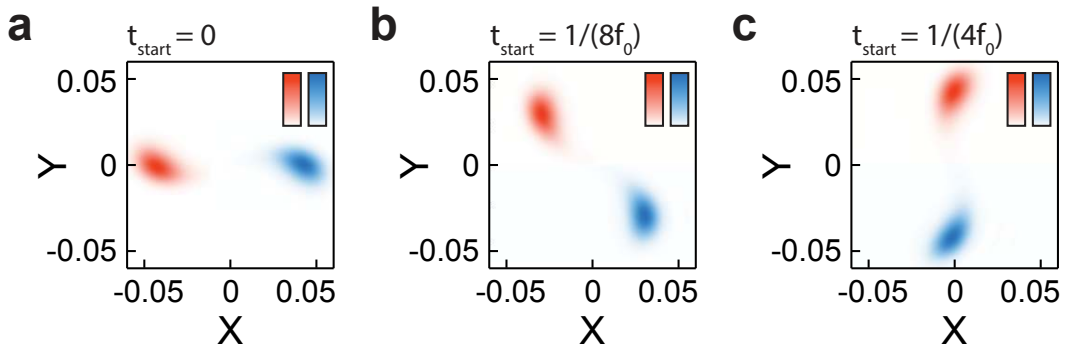


Figure S5: Fokker-Planck simulation of the potential deformation protocol with noise. The three subfigures correspond to flipping protocols that start at different times t_{start} within the oscillation cycle. The pulse length is set to the optimal value $\tau_{\text{def}} = 1/f_0$. Each panel combines the initial (red) and the final (blue) state in a single graph. (a) Potential deformation phase flip initialized at $t_{\text{start}} = 0$ when resonator has maximum displacement and minimum momentum. This is the same data as in Figs. S4a and c. (b) Potential deformation phase flip initialized at time $t_{\text{start}} = 1/(8f_0)$, when resonator has equal (normalized) displacement and momentum. (c) Potential deformation phase flip initialized at time $t_{\text{start}} = 1/(4f_0)$, when the resonator has minimum displacement and maximum momentum. The colorbars range from $p = 0$ (white) to $p = 4850$ (red/blue).

B. Numerical results: Potential deformation

We now numerically investigate the method termed ‘potential deformation’ introduced in the main text, where it was implemented with the levitated nanoparticle. To this end, starting with the distribution $p_{\text{ini}}(X, Y, t = 0)$, we switch the potential to $\omega_0 = 0.5$ during the flip time τ_{def} . In Fig. S4, we show the results of our simulations for an optimal pulse length $\tau_{\text{def}} = 1/f_0$. The time $t = 0$ where the pulse starts is chosen such that the resonator has maximum (negative) displacement and minimum momentum. (Note that this is the situation that we experimentally realized.) In the different panels, we show snapshots of $p(X, Y, t)$ at the beginning ($t = 0$, panel a), in the middle [$t = 1/(2f_0)$, panel b], and at the end ($t = 1/f_0 = \tau_{\text{def}}$, panel c) of the deformation pulse. We observe that the probability distribution is slightly distorted during the pulse (see panel b). However, at the end of the pulse, the phase-space distribution is essentially indistinguishable from the starting distribution, except that it has been rotated by π in phase space.

Having found that our phase-flip protocol based on potential deformation retains the shape of the initial phase-space distribution, we further investigate the robustness of our method to variations in the starting time of the pulse. In Fig. S5, we show the results of Fokker-Planck simulations of rapid phase flips for different starting times t_{start} of the potential-deformation pulse during the oscillation cycle of the parametron. In each panel, we show the starting distribution $p_{\text{ini}}(X, Y, t_{\text{start}})$ in red, together with the distribution $p_{\text{ini}}(X, Y, t_{\text{start}} + \tau_{\text{def}})$ in blue. Here, we have chosen the ideal pulse length $\tau_{\text{def}} = 1/f_0$. Note that Fig. S5a contains the combined information of Fig. S4a and c. Interestingly, looking at Fig. S5, we observe no appreciable difference in the resulting phase state as we vary the starting time of the pulse through the oscillation period of the parametron. These findings are in agreement with our expectation: During the time $\tau_{\text{def}} = 1/f_0$, which corresponds to half an oscillation period in the deformed potential, the phase state of the oscillator inverts, i.e., it evolves from (X, Y) to $-(X, Y)$, irrespective of the starting state. Accordingly, our bit-flip protocol based on potential deformation can be executed at any arbitrary point in time throughout the parametron oscillation cycle. Furthermore, our results show that the phase-flip protocol based on potential deformation leaves the width of the phase-space distribution essentially unchanged. Consequently, we conclude that the protocol is robust against inevitable additive force noise which can arise due to coupling to a thermal bath.

[S1] J. Gieseler, B. Deutsch, R. Quidant, and L. Novotny, Phys. Rev. Lett. **109**, 103603 (2012).

[S2] J. Gieseler, L. Novotny, and R. Quidant, Nature Physics **9** (2013).

[S3] V. Jain, J. Gieseler, C. Moritz, C. Dellago, R. Quidant, and L. Novotny, Phys. Rev. Lett. **116**, 243601 (2016).

[S4] J. Gieseler, R. Quidant, C. Dellago, and L. Novotny, Nature Nanotechnology **9**, 358 (2014).

[S5] Z. Nosan, P. Märki, N. Hauff, C. Knaut, and A. Eichler, Phys. Rev. E **99**, 062205 (2019).

[S6] C. Gardiner, *Stochastic Methods*, Springer-Verlag Berlin Heidelberg (2009).